AIP | Applied Physics Letters

Intrinsic beam shaping mechanism in spatially modulated broad area semiconductor amplifiers

Mindaugas Radziunas, Muriel Botey, Ramon Herrero, and Kestutis Staliunas

Citation: Appl. Phys. Lett. **103**, 132101 (2013); doi: 10.1063/1.4821251
View online: http://dx.doi.org/10.1063/1.4821251
View Table of Contents: http://apl.aip.org/resource/1/APPLAB/v103/i13
Published by the AIP Publishing LLC.

Intrinsic beam shaping mechanism in spatially modulated broad area semiconductor amplifiers

Mindaugas Radziunas,[1] Muriel Botey,[2] Ramon Herrero,[3] and Kestutis Staliunas[3,4]
[1]*Weierstrass Institute for Applied Analysis and Stochastics, Leibniz Institute in Forschungsverbund Berlin e.V., Mohrenstrasse 39, 10117 Berlin, Germany*
[2]*Departament de Física i Enginyeria Nuclear, Universitat Politècnica de Catalunya, Urgell 187, 08036 Barcelona, Spain*
[3]*Departament de Física i Enginyeria Nuclear, Universitat Politècnica de Catalunya, Colom 11, 08222 Terrassa, Spain*
[4]*Institució Catalana de Recerca i Estudis Avançats (ICREA), Pg. Lluis Companys 23, 08010 Barcelona, Spain*

(Received 24 May 2013; accepted 18 July 2013; published online 23 September 2013)

We investigate beam shaping in broad area semiconductor amplifiers induced by a 2-dimensional (longitudinal and lateral) periodic modulation of the pump on a scale of several microns. The study is performed by solving numerically a $(2+1)$-dimensional model for the semiconductor amplifier. We show that, under realistic conditions, the anisotropic gain induced by the pump periodicity can show narrow angular profile of enhanced gain of less than 1°, providing an intrinsic filtering mechanism and eventually improving the spatial beam quality. © *2013 AIP Publishing LLC*. [http://dx.doi.org/10.1063/1.4821251]

Edge emitting broad area semiconductor (BAS) lasers are relevant light sources due to their numerous applications. Their particular geometry (planar configuration) provides high conversion efficiency, as the pump efficiently accesses the entire volume of the active amplifying medium. The main disadvantage of BAS lasers is the relatively low spatial and temporal quality of the emitted beam[1,2] due to the absence of an intrinsic selection mechanism within its large aspect-ratio cavity. In addition, the Bespalov-Talanov modulation instability in strongly nonlinear regimes may lead to filamentation and additionally deteriorate the quality of the beam.[3] The multi-transverse mode operation results in a strong divergence of the emitted beam. The large beam quality factor M^2, i.e., the large deviation of such a beam from the diffraction limited Gaussian,[4] among others, prevents coupling into optical fibers which precludes such lasers from many other important applications.

The typical divergence of BAS lasers emission (3–5 mm long, 200 μm wide, and wavelength around 1 μm) ranges from 5° to 10°. A great challenge would be to reduce such divergence to much less than 1°, i.e., closer to the diffraction limit (that is 0.1° for a 200 μm wide beam). Several approaches have been proposed and applied to improve the spatial quality of the radiation, each, however, with its disadvantages. For example, different schemes of optical injection[5,6] and optical feedback,[7,8] or integrated narrow master oscillator—tapered power amplifier configurations[9,10] improve the beam quality, however, in return, the laser becomes less compact or is rather sensitive to the back reflections.

Recently, novel techniques have been proposed to improve the spatial quality of the beams implementing a spatial (or angular) filtering mechanism in materials with spatially modulated refractive index on the wavelength scale. Photonic Crystals (PhCs) apart from being well-known for tailoring frequency dispersion[11] can also display angular band-gaps.[12] The angular positions of such band-gaps depend, among others, on the geometry of the modulation, i.e., on the longitudinal and transverse periods of the PhC, $d_{||}$ and $d_{\perp}$, respectively. A dimensionless geometric parameter $\mathcal{Q} = 2d_{\perp}^2 n_b/(\lambda_0 d_{||})$ determines the character of spatial dispersion, where λ_0 is the considered beam wavelength in vacuum, and n_b is the background refractive index. Hence, a proper selection of the geometry, satisfying $\mathcal{Q} \approx 1$, sets angular band-gaps at small angles from the optical axis direction, whereas the on-axis radiation lays in propagation bands. This results in a low-angle-pass filter recently proposed and demonstrated not only in optics[12–15] but also in acoustics (by so called Sonic Crystals).[16,17]

On the other hand, materials with periodically in space modulated gain have recently shown to provide anisotropic amplification profile.[18,19] The maximum amplification is obtained for beams propagating along the crystallographic axes of the modulated structure, for the geometry factor $\mathcal{Q} = 1$, similar to PhCs angular filters. Physically, anisotropic gain for specific Bloch modes of the radiation (for a given frequency and propagation direction) is obtained when their field maxima coincide with the spatial areas of maximum gain. Therefore, such modes are more amplified than non-resonant Bloch waves or than plane waves in a homogeneous (averaged) gain medium.

We propose here to combine both gain and index modulation (GIM) in order to obtain three in one: amplification, angular filtering, and eventually improvement of the spatial structure of the beam. It has been recently proposed that a resulting anisotropic gain could be used in BAS lasers and amplifiers,[20] where the proof-of-principle calculations were performed on a simplified model. The aim of the present work is to verify whether the scheme is indeed applicable to actual BAS amplifiers with realistic parameters of today-available semiconductor materials. Additional purpose is to quantify the predicted effect and to calculate the angular width of the enhanced amplification profile. We also note that although the object of our study is not a BAS laser but a BAS amplifier, we expect that a strongly anisotropic gain in

the amplifier would mean improving the beam structure of lasers too.

There are various possibilities to spatially modulate the BAS amplifier, such as using spatially modulated electrodes for electric pumping (as considered in the present letter) or micro-structuring the amplifying media (e.g., etching periodic arrays of holes, and possibly filling them by media with desired refraction properties). Throughout this letter, we consider a simple chess-box shape of the electrodes, as illustrated in Fig. 1, for a better adaptation to numerical simulations. The filtering performance is essentially sensitive to the modulation periodicities rather than to the specific distribution within the unit cell. Moreover, the diffusion of carriers smoothens any sharp distribution into almost a harmonic modulation.[20]

A narrow beam of a width $20\,\mu$m and corresponding divergence of 1° is injected into such a single-pass amplifier. The periodic distribution of gain in the transverse direction results in splitting the transmitted beam into at least three diffracted components as shown in Fig. 1: a central beam and two symmetrically positioned diffraction beams, propagating at angles $\pm\varphi(d_\perp)$. Due to the resonant interplay between transverse and longitudinal modulations of the amplifying medium, which occurs at $\mathcal{Q}\approx 1$, these three field harmonics interact, and as a result, anisotropic gain develops. In particular, we assume $\lambda_0 = 1\,\mu$m, $n_b \approx 3.125$, and in most cases $d_\perp = 8\,\mu$m, $d_{||} = 400\,\mu$m, which fulfill the above resonance condition. The free-space diffraction angle for this case is $\varphi \approx 7.2^\circ$. In order to determine the optimum angular filtering performance, we scan the $\mathcal{Q}$ parameter in a range around 1.

We use a $2+1$-dimensional traveling wave model approach,[10,21,22] where the spatio-temporal dynamics of the optical field is governed by the following set of equations:

$$\begin{aligned}
&\left[\frac{n_g}{c_0}\partial_t + \partial_z + \frac{i}{2k_0 n_b}\partial_x^2\right]E = [\beta(N,|E|^2) - \mathcal{D}]E,\\
&\mathcal{D}E = \frac{\bar{g}}{2}(E-P), \quad \partial_t P = \bar{\gamma}(E-P) + i\bar{\omega}P,\\
&E(0,x,t) = a(x,t) = \sqrt{\frac{2n_g\lambda_0}{\sigma d h c_0^2}}\sqrt{\frac{\ln 2}{\pi}}\mathcal{P}\, e^{i\omega t - \frac{x^2\ln 4}{\sigma^2}},
\end{aligned} \tag{1}$$

here $E(z,x,t)$ is the slowly varying complex amplitude of the optical field propagating along the longitudinal axis of the BAS amplifier, $|E|^2$ denotes a local photon density, the linear operator $\mathcal{D}$, and the induced polarization function $P(z,x,t)$ model the Lorentzian approximation of the material gain dispersion,[23] whereas the complex function $a(x,t)$ represents an optically injected Gaussian beam of power $\mathcal{P}$. The complex propagation factor,

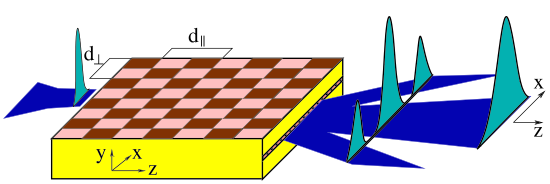

FIG. 1. Planar semiconductor amplifier structure with chess-box electrodes. The pump profile is periodically modulated in space, with longitudinal and transverse periods $d_{||}$ and $d_\perp$.

$$\beta(N,|E|^2) = -\frac{\alpha}{2} + \frac{g(N,|E|^2)}{2} + i\,\tilde{n}(N), \tag{2}$$

couples the field to the carrier density $N(z,x,t)$ governed by

$$\begin{aligned}
[\partial_t - d_N\partial_x^2]N = {}& \frac{\bar{J}\cdot\zeta(z,x)}{qd} - (AN + BN^2 + CN^3)\\
&- \frac{c_0}{n_g}\Re e[E^*(g(N,|E|^2) - 2\mathcal{D})E].
\end{aligned} \tag{3}$$

The gain, the index change, and the spatial current modulation functions g, $\tilde{n}$, and ζ are defined as

$$\begin{aligned}
&g(N,|E|^2) = \frac{g'\ln(N/N_{\rm tr})}{1+\varepsilon|E|^2}, \quad \tilde{n}(N) = k_0\sqrt{\nu N},\\
&\zeta(z,x) = 1 + \mathrm{sign}[\sin(2\pi z/d_{||})\sin(2\pi x/d_\perp)].
\end{aligned} \tag{4}$$

We use the following parameters: group velocity index $n_g = 3.6$, depth of the active zone $d = 15$ nm, differential gain $g' = 25\,\mathrm{cm}^{-1}$, refractive index change factor $\nu = 10^{-25}\,\mathrm{cm}^3$, transparency carrier density $N_{\rm tr} = 10^{18}\,\mathrm{cm}^{-3}$, internal absorption $\alpha = 1.5\,\mathrm{cm}^{-1}$, nonlinear gain compression $\varepsilon = 5\times 10^{-18}\,\mathrm{cm}^3$, carrier diffusion coefficient $d_N = 21\,\mathrm{cm}^2/\mathrm{s}$, recombination parameters $A = 0.3/\mathrm{ns}$, $B = 2\times 10^{-10}\,\mathrm{cm}^3/\mathrm{s}$, and $C = 2.5\times 10^{-30}\,\mathrm{cm}^6/\mathrm{s}$, Lorentzian gain amplitude $\bar{g} = 100\,\mathrm{cm}^{-1}$, half width at half maximum $\bar{\gamma} = 60/\mathrm{ps}$, gain peak detuning $\bar{\omega} = 0/\mathrm{ps}$, full width at half maximum of the optical injection intensity $\sigma = 20\,\mu$m, and mean injection current density $\bar{J} = 10\,\mathrm{A/mm}^2$. The frequency of the optical injection ω is set to zero. Finally, c_0, q, h, and $k_0 = \frac{2\pi}{\lambda_0}$ are the speed of light in vacuum, electron charge, Planck constant, and reference wave-number, respectively. Some of these parameters are non-homogeneous, particularly, the function $\bar{J}\zeta(z,x)$ corresponds to the pump current density, which equals $2\bar{J}$ at the simulated periodic contacts and 0 elsewhere. The spatially modulated current is responsible for the modulation of the carrier density of the propagation factor β, and therefore, for the gain and index modulation within the BAS amplifier. More details on the specific meaning and typical values of all parameters given above can be found in Ref. 10.

The basic results are summarized in Figs. 2 and 3. Fig. 2 presents a comparison between BAS amplifiers with uniform and modulated pump. For a weak injected beam and short propagation distances ($\mathcal{P} = 0.1$ mW and $z < 2$ mm), the propagating field power is not sufficient for a significant saturation of the gain, i.e., it has a minor impact on carrier distribution determined by the stationary Eq. (3) (see the orange curves in panels (i) and (j) and panels (c) and (d) for $z < 2$ mm). The locally averaged carrier density as well as its modulation amplitude remain almost constant over all the width of the amplifier. Hence, the distribution of the propagation factor $\beta(z,x)$ in Eq. (1) remains defined by the stationary N. The beam intensity grows exponentially [see panels (g) and (h) for $z < 2$ mm] and is governed by the *linear* field equation (1) with the spatially periodic potential β. In this linear regime, the far field does not change.

For $z > 2$ mm, the amplified field starts to deplete the carrier density [see panels (c) and (d)], which results in the saturation of the emitted field intensity [see panels

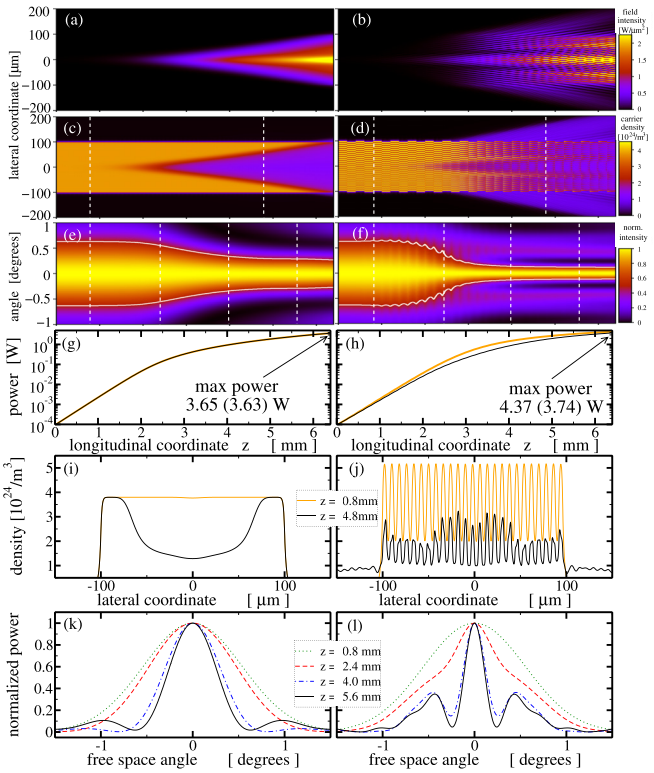

FIG. 2. Amplification of the beam in 200 μm-wide BAS amplifiers for uniform pump [left column], and for periodically modulated pump with $\mathcal{Q} = 1.02\,(n_b = 3.1875)$ [right column]. From top to bottom: power ((a) and (b)); carrier densities ((c) and (d)); central part of the far field, with half maxima indicated by white contour lines ((e) and (f)); evolution of the intensity of the field [orange] and its part within the central $\pm 2.5^\circ$ segment [black] ((g) and (h)). (a)–(h) plotted as a function of the propagation distance, z. The carrier density and the far fields at the dashed white vertical lines of panels (c), (d), (e), and (f) are shown in panels (i), (j), (k), and (l), respectively.

(g) and (h)]. The amplitude of the spatial modulation of the carriers is no more uniform [see black curves in panels (i) and (j)], what is beyond the linear analysis of Ref. 20. However, the predicted effects remain valid: the optical field in the modulated case develops significant side-bands at the angles $\pm\varphi(d_\perp)$, and the central far field lobe is squeezed down to $\sim 0.25^\circ$ [compare far fields for $z = 4.0$ and 5.6 mm in panels (k) and (l) and panels (e) and (f) for $z > 2$ mm].

The left column of Fig. 3 depicts the amplification properties of 4.8 mm-long devices for different values of $\mathcal{Q}$. The amplifier shows a strong narrowing of the central part of the far field for $\mathcal{Q} \in [1.01, 1.1]$ (see the contour lines in panel (a), indicating the width of the central far field lobe). The far field contains diffraction components at $\pm\varphi(8\,\mu\text{m}) \approx \pm 7.2^\circ$ [panel (e)].

For comparison, we have simulated a two times broader amplifier with the same modulation periods and same injected current density, as shown in the right column panels of Fig. 3. The narrowing of the central part of the far field is more efficient in the latter case [$\mathcal{Q} \in [1, 1.05]$ in panel (b)]; however, the radiation into diffraction components is also more pronounced [panel (f)] resulting in smaller part of the total radiation within the central segment [compare panels (c) and (d)]. This dependence on the width of the device is due to different amplification and reflection of the sidelobe radiation from the (lateral) grating generated by the periodic pump.

In Fig. 4, we summarize our results for modulated BAS amplifiers with different modulation periods. In all cases, periods $d_\perp$ and $d_\parallel$ are chosen such that $\mathcal{Q} = 1.02$. It is obvious that in the case of the smallest periods $d_\perp = 4\,\mu$m and $d_\parallel = 100\,\mu$m (black dotted curves) the compression of the central part of the far field is less pronounced [see panel (d) and panel (a) for $z \le 3.5$ mm] and also side lobes arise increasing the beam width at half maximum [see panels (d)–(f) and (a) for $z > 3.5$ mm]. This can be explained by insufficient contrast of the GIM in unsaturated devices: whereas the locally averaged value of carriers $\langle N \rangle$ (and consequently, of gain and refractive index) in all considered cases is determined by the mean injected current $\bar{J}$ ($\langle N \rangle \approx \frac{\bar{J}}{qdA}$ for a linear approximation of the carrier recombination), the carrier modulation amplitude ΔN (and, consequently, the GIM amplitudes) strongly depends on the lateral

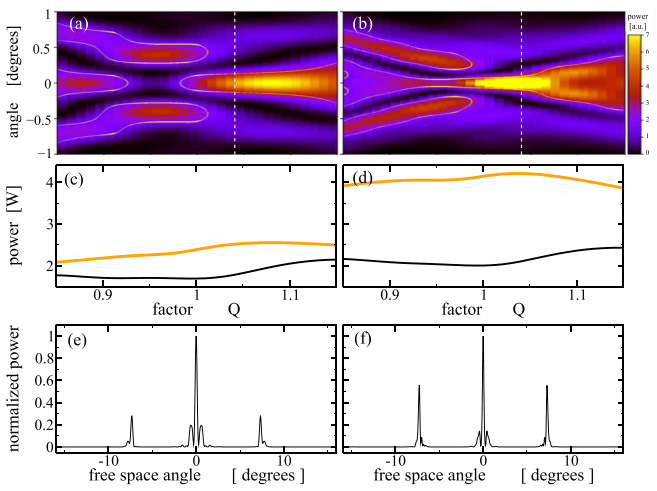

FIG. 3. Amplification of the beam with $\sigma = 20\,\mu$m for a $L = 4.8$ mm long BAS amplifiers with periodical pump and two different device widths: 200 μm [left column], 400 μm [right column]. From top to bottom: central part of the far fields with half maxima indicated by light contour lines ((a) and (b)); power of the transmitted field [orange] and corresponding central part within $\pm 2.5^\circ$ [black] ((c) and (d)). (a)–(d) Plotted as a function of $\mathcal{Q}$. The far fields for $\mathcal{Q} = 1.02$ [dashed white vertical lines in panels (a) and (b)] are shown in panels (e) and (f).

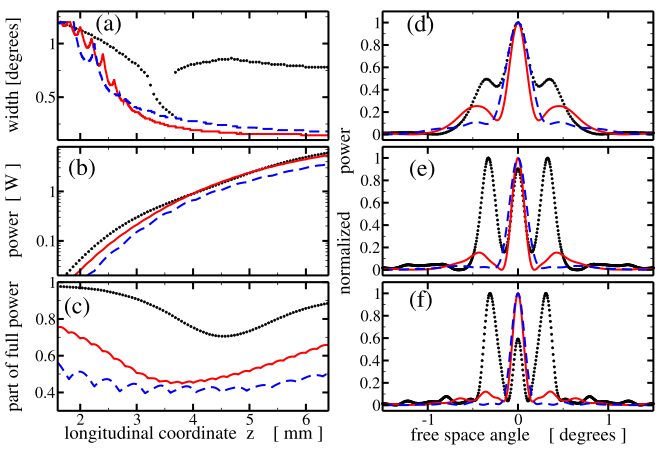

FIG. 4. Amplification of the beam in 400 μm wide BAS amplifiers with modulated pump with $d_\perp = 4\,\mu$m, $d_\parallel = 100\,\mu$m (black dot), $d_\perp = 8\,\mu$m, $d_\parallel = 400\,\mu$m (red solid), $d_\perp = 12\,\mu$m, $d_\parallel = 900\,\mu$m (blue dash). In all three cases, $\mathcal{Q} = 1.02$. (a): width of the central far field part at the half maximum. (b) and (c): intensity of the emitted field within the central $\pm 2.5^\circ$ segment and its part within the full emitted field intensity. (d)–(f): central part of the far fields at $z = 3.2$ mm, $z = 4.8$ mm, and $z = 6.4$ mm, respectively.

period $d_\perp$ of the modulated contact: $\Delta N \approx \frac{4\bar{J}/(\pi q d)}{A+4\pi^2 d_N/d_\perp^2}$. This is due to a significant contribution of the carrier diffusion, which smoothens effectively the carrier distribution in devices with small modulation periods. Note also the appearance of the side lobes of the far field at $\pm 0.4^\circ$ angles [black dotted curves in panels (d)–(f)], which we attribute to the modulation instability typical for BAS amplifiers without modulation. Increasing the periods of modulation, these side lobes are suppressed, and the central part of the far field is compressed down to $\sim 0.2^\circ$. On the contrary, increasing the periods of the modulation has also some drawbacks, since the optical field radiated at the angles $\pm\varphi(d_\perp)$ increases. Whereas for the case of $d_\perp = 4\,\mu$m, the amount of field radiated within the central $\pm 2.5^\circ$ segment is larger than 70%, for $d_\perp = 12\,\mu$m it is less than 50% [see panel (c)], and the absolute value of this intensity is significantly lower [blue dashed curve in panel (b)]. It seems that optimal choice of modulation periods is $d_\perp \approx 8\,\mu$m. Even though the side angle radiation is still large [red solid curve in panel (c)], the absolute amount of the emitted field within the central segment is comparable or even larger than that one in the GIM amplifier with $d_\perp = 4\,\mu$m [panel (b)], whereas the central lobe of the far field is significantly compressed [panels (d)–(f)].

To conclude, we show that a spatial modulation of the bias current in BAS amplifiers with a length on the order of a few millimeters can lead to a substantial improvement of the spatial structure of the amplified beam. The study is performed under realistic semiconductor parameters and technically realizable modulation periods. Since in this study we have considered amplification of a perfect Gaussian incident beam with $M^2 = 1$, we do not discuss the improvement of the beam quality, as it is already maximal at the entrance of the amplifier. However, the beam quality strongly increases when we consider a random beam of the same angular width at the entrance.[20] A more detailed study of the noisy beam amplification, however, is out of the scope of this letter. Beyond what is here presented, this new technique could be implemented to improve the spatial quality of emission of BAS lasers.

We acknowledge financial support of Spanish Ministerio de Educación y Ciencia and European FEDER (Project No. FIS2011-29734-C02-01). The work of M. Radziunas was supported by DFG Research Center Matheon.

[1]T. Burkhard, M. Ziegler, I. Fischer, and W. Elsäßer, Chaos, Solitons Fractals **10**, 845 (1999).
[2]H. Adachihara, O. Hess, E. Abraham, P. Ru, and J. Moloney, J. Opt. Soc. Am. B **10**, 658 (1993).
[3]V. I. Bespalov and V. I. Talanov, "Filamentary structure of light beams in nonlinear liquids," JETP Lett. **3**, 307 (1966) [Pis'ma Zh. Eksp. i Teor. Fiz. **3**, 471, (1966)].
[4]A. Siegman, Proc. SPIE **1868**, 2–12 (1993).
[5]L. Goldberg and M. Chun, Appl. Phys. Lett. **53**, 1900 (1988).
[6]M. Radziunas and K. Staliunas, Europhys. Lett. **95**, 14002 (2011).
[7]V. Raab and R. Menzel, Opt. Lett. **27**, 167 (2002).
[8]S. Mandre, I. Fischer, and W. Elsäßer, Opt. Lett. **28**, 1135 (2003).
[9]B. Sumpf, K.-H. Hasler, P. Adamiec, F. Bugge, F. Dittmar, J. Fricke, H. Wenzel, M. Zorn, G. Erbert, and G. Trankle, IEEE J. Sel. Top. Quantum Electron. **15**, 1009 (2009).
[10]M. Spreemann, M. Lichtner, M. Radziunas, U. Bandelow, and H. Wenzel, IEEE J. Quantum Electron. **45**, 609 (2009).
[11]*Photonic Crystals and Light Localization in the 21st Century, NATO Science Series C*, edited by C. Soukoulis (Kluwer Academic Publisher, 2001), Vol. 563.
[12]E. Colak, A. Cakmak, A. Serebryannikov, and E. Ozbay, J. Appl. Phys. **108**, 113106 (2010).
[13]K. Staliunas and V. Sánchez-Morcillo, Phys. Rev. A **79**, 053807 (2009).
[14]L. Maigyte, T. Gertus, M. Peckus, J. Trull, C. Cojocaru, V. Sirutkaitis, and K. Staliunas, Phys. Rev. A **82**, 043819 (2010).
[15]V. Purlys, L. Maigyte, D. Gailevičius, M. Peckus, M. Malinauskas, and K. Staliunas, Phys. Rev. A **87**, 033805 (2013).
[16]R. Picó, V. Sánchez-Morcillo, I. Pérez-Arjona, and K. Staliunas, Appl. Acoust. **73**, 302 (2012).
[17]R. Picó, I. Pérez-Arjona, V. Sánchez-Morcillo, and K. Staliunas, Appl. Acoust. **74**, 945 (2013).
[18]K. Staliunas, R. Herrero, and R. Vilaseca, Phys. Rev. A **80**, 013821 (2009).
[19]M. Botey, R. Herrero, and K. Staliunas, Phys. Rev. A **82**, 013828 (2010).
[20]R. Herrero, M. Botey, M. Radziunas, and K. Staliunas, Opt. Lett. **37**, 5253 (2012).
[21]S. Balsamo, F. Sartori, and I. Montroset, IEEE J. Sel. Top. Quantum Electron. **2**, 378 (1996).
[22]A. Egan, C. Ning, J. Moloney, R. Indik, M. Wright, D. Bossert, and J. McInerney, IEEE J. Quantum Electron. **34**, 166 (1998).
[23]U. Bandelow, M. Radziunas, J. Sieber, and M. Wolfrum, IEEE J. Quantum Electron. **37**, 183 (2001).